PHYSICAL REVIEW B VOLUME 26, NUMBER 12 15 DECEMBER 1982

Dynamic transmission and reflection phenomena for a time-dependent rectangular potential

D. L. Haavig and R. Reifenberger
Department of Physics, Purdue University, West Lafayette, Indiana 47907
(Received 4 March 1982)

The time-dependent Schrödinger equation is solved for a one-dimensional rectangular potential whose height changes sinusoidally in time. By using standard wave-matching techniques, dynamic transmission and reflection probabilities are found. It is shown that the flux transmitted through the barrier region is modulated in time at integer multiples of ω_b, the angular frequency at which the potential oscillates. The results obtained for a delocalized plane wave incident on the barrier are extended by considering the interaction of a Gaussian wave packet with the oscillating potential barrier. The modulation of the transmitted and reflected probability density by the oscillating barrier is clearly demonstrated by a series of calculations performed to illustrate this interaction. These calculations also show that the probability density leaving the barrier region is composed of individual wave packets having different average velocities, a result which is a direct consequence of the transitions induced by the time-dependent potential barrier under consideration. Calculations are also performed which show that the flux transmitted across the potential barrier depends on the phase of the oscillating barrier at the time the incident Gaussian wave packet begins to interact with it. The results of these model calculations suggest that experiments properly designed to measure the transmission probability of a quantum particle as it escapes from a metal surface are likely to provide information about the time formation of the dynamic image potential.

I. INTRODUCTION

Although much attention has been given to a calculation of the transmission and reflection probabilties through potential barriers of arbitrary shape, little consideration has been devoted to a similar calculation in which the shape of the potential barrier depends on time. In this paper, we discuss the interaction of a quantum-mechanical particle with a one-dimensional potential barrier of finite width whose magnitude is a sinusoidal function of time.[1] This dynamic interaction is analyzed using two different initial states to emphasize both the analytic results obtained for a delocalized incident plane wave and also the time evolution observed for a traveling Gaussian wave packet that interacts with the model potential barrier. The results of this paper are important because they extend in a straightforward fashion the standard discussions of time-independent rectangular potential barriers found in most quantum-mechanics texts.[2] More importantly, the calculations are also a useful first step toward understanding the physical principles involved in the more general problem of calculating the transmission probability of a particle across a time-dependent potential barrier of arbitrary shape.

The contents of this paper are closely related to the design of experiments that measure the time evolution of the dynamic image potential. As is well established from theoretical considerations, a quantitative calculation of the image potential must be based in some way on a model which properly takes into account the past trajectory of a charged particle as it moves in the vicinity of a metal surface. A question that must be asked in order to measure the actual properties of this dynamic image potential is what effects, if any, will the dynamic potential have on the motion of a quantum-mechanical particle. In this regard, it is worthwhile to consider the case of an electron that escapes from a metal surface and to ask whether the transmission of this electron across a dynamic surface potential barrier is the same or different from the case when dynamic effects are neglected. We show in this paper that a simple model for a dynamic potential barrier will produce, under certain circumstances, a measurable effect on the transmission probability. By answering the above question in the affirmative, we are attempting to (1) develop a framework to analyze the effects of the transmission of quantum particles through a time-dependent potential, and (2) solve the problem for a simple model in order to provide qualitative guidelines to aid in the design of experiments that measure the physical properties of

the dynamic image potential.

Questions concerning dynamic potential barriers have been a topic of interest in a number of recent papers in solid state physics.[3–5] In particular, the suggestion was made in Ref. 5 that electrons photoemitted at energies below threshold from a metal surface in the presence of a strong applied electric field are especially sensitive to the details of the dynamic image potential. Following the suggestions made in Ref. 5, we demonstrate in what follows that the time dependence inherent in a dynamic potential should modulate the transmission probability for quantum-mechanical particles.

This paper is organized in the following way. In order to provide insight into the dynamics of a particle interacting with an oscillating barrier, we derive, in Sec. II, the reflection and transmission probabilities of a delocalized quantum particle interacting with a time-dependent rectangular barrier. The physical principles discussed in Sec. II are extended to a localized quantum particle in Sec. III. In this section we modify the algorithm developed by Goldberg, Schey, and Schwartz[6] (GSS) and use it to generate computer plots of a Gaussian wave packet incident upon a time-dependent potential. The modified algorithm is used to calculate the time evolution of the wave packet under various circumstances and computer plots of this dynamic interaction are presented. A calculation is performed that illustrates the importance of the phase of the oscillating barrier at the time when a quantum particle interacts with it. In Sec. IV, we provide a brief discussion of the salient features of our results.

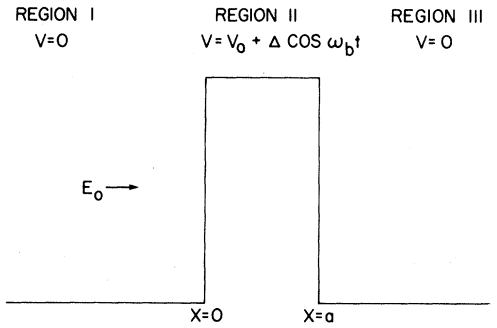

FIG. 1. Schematic diagram of the potential barrier used for the exact calculation of reflection and transmission probabilities of a quantum particle of energy E_0 incident on the barrier. The barrier changes its magnitude sinusoidally in time about its average value of V_0 with angular frequency ω_b and amplitude Δ.

II. EXACT SOLUTION FOR TRANSMISSION AND REFLECTION PROBABILITIES

The exact solution for the reflection and transmission probabilities of a quantum particle with energy E_0 incident on a time-dependent potential barrier requires the solution of the time-dependent Schrödinger equation ($\hbar=1$, $m=\frac{1}{2}$):

$$H(x,t)\psi(x,t)=i\frac{\partial}{\partial t}\psi(x,t) ,$$

where

$$H(x,t)=\frac{\partial^2}{\partial x^2}+V(x,t)=H_0+V(x,t) . \tag{1}$$

Our model for $V(x,t)$ is specified by (see Fig. 1)

$$V(x,t)=V_1(x)+V_2(t)=\begin{cases}0 & \text{for } x\le 0\\ V_0+\Delta\cos(\omega_b t) & \text{for } 0<x<a\\ 0 & \text{for } x\ge a .\end{cases} \tag{2}$$

Since the Schrödinger equation is separable in the space and time coordinates for $V(x,t)$ given by Eq. (2), the wave function can be expressed as a product of a position-dependent function and a time-dependent function: $\psi_j(x,t)=\phi_j(x)a_j'(t)$. Direct substitution of this wave function into the Schrödinger equation gives

$$H_0\phi_j(x)+V_1(x)\phi_j(x)=E_j\phi_j(x) , \tag{3}$$

$$a_j'(t)=a(t)e^{-iE_jt}$$

$$=e^{-i\int V_2(t')dt'}e^{-iE_jt} , \tag{4}$$

where E_j is the separation constant and has units of energy. The most general form for the wave function is a summation over all states characterized by E_j:

$$\psi(x,t)=\sum_j a(t)\phi_j(x)e^{-i\omega_j t} , \tag{5}$$

where $\omega_j=E_j$ ($\hbar=1$). The discrete summation over all possible states E_j in Eq. (5), rather than the more appropriate integral over all E_j, is employed for notational simplicity in anticipation of results presented later in this section. The approach that we adopt here is to solve Eq. (1) for each of the three regions defined in Eq. (2) with the wave function for each region given by Eq. (5). The transmission and re-

flection probabilities that are of major interest can then be obtained by suitable wave-matching techniques. The general solution equations (3) and (4) will now be discussed for the model poential barrier under consideration.

A. Wave functions

The solution of Eq. (3) in regions I and III has the form

$$\phi_j(x)=\Theta(E_j)(T_j e^{ik_j x}+R_j e^{-ik_j x}) +\Theta(-E_j)(R_j' e^{k_j x}+T_j' e^{-k_j x}) , \quad (6)$$

with

$$k_j=|E_j|^{1/2} , \quad (7)$$

and where

$$\Theta(E)=0 \text{ for } E<0$$

$$\Theta(E)=1 \text{ for } E>0 .$$

For $x\leq 0$ (region I), the potential is time independent and Eq. (4) gives $a_j(t)=1$. Since the wave function must remain finite for all x, the coefficients T_j' in Eq. (6) must be set to zero. Also, since it is assumed that a quantum particle of incident energy E_0 is traveling toward $x=+\infty$, T_j in Eq. (6) equals zero unless $k_j=k_0$. Thus the wave function in region I must be given by

$$\Psi_{\rm I}(x,t)=e^{ik_0 x}e^{-i\omega_0 t}+\sum_j \Theta(E_j)R_j e^{-ik_j x}e^{-i\omega_j t} +\sum_j \Theta(-E_j)R_j' e^{k_j x}e^{-i\omega_j t} , \quad (8)$$

where

$$k_0=E_0^{1/2} \text{ and } \omega_0=E_0 .$$

The general solution of Eq. (3) in region II has the form

$$\phi_j(x)=A_j e^{\kappa_j x}+B_j e^{-\kappa_j x} , \quad (9)$$

with

$$\kappa_j=[V_0(x)-E_j]^{1/2} . \quad (10)$$

In this region, $a_j(t)$ is found from Eq. (4) to be

$$a_j(t)=e^{-i\alpha \sin(\omega_b t)} , \quad (11)$$

where $\alpha=\Delta/\omega_b$. Using this result with Eq. (9) gives

$$\Psi_{\rm II}(x,t)=\sum_j (A_j e^{\kappa_j x}+B_j e^{-\kappa_j x})e^{-i\omega_j t}e^{-i\alpha \sin(\omega_b t)} . \quad (12)$$

Lastly, for region III, the $a_j(t)$ from Eq. (4) are again equal to unity. Further, for the wave function to remain finite at large x, the coefficients R_j' in Eq. (6) must be set to zero. Thus the wave function for a transmitted wave in region III is

$$\Psi_{\rm III}=\sum_j \Theta(E_j)T_j e^{ik_j x}e^{-i\omega_j t} +\sum_j \Theta(-E_j)T_j' e^{-k_j x}e^{-i\omega_j t} . \quad (13)$$

B. Wave matching

To be physically acceptable the wave function and its derivative must be continuous throughout all space. To satisfy this constraint, the following four matching equations must be satisfied:

$$e^{-i\omega_0 t}+\sum_j \Theta(E_j)R_j e^{-i\omega_j t}+\sum_j \Theta(-E_j)R_j' e^{-i\omega_j t} =\sum_j (A_j+B_j)e^{-i\omega_j t}e^{-i\alpha \sin(\omega_b t)} , \quad (14)$$

$$ik_0 e^{-i\omega_0 t}+\sum_j \Theta(E_j)(-ik_j)R_j e^{-i\omega_j t} +\sum_j \Theta(-E_j)k_j R_j' e^{-i\omega_j t} =\sum_j (A_j\kappa_j-B_j\kappa_j)e^{-i\omega_j t}e^{-i\alpha \sin(\omega_b t)} , \quad (15)$$

$$\sum_j \Theta(E_j)T_j e^{ik_j a}e^{-i\omega_j t}+\sum_j \Theta(-E_j)T_j' e^{-k_j a}e^{-i\omega_j t} =\sum_j (A_j e^{\kappa_j a}+B_j e^{-\kappa_j a})e^{-i\omega_j t}e^{-i\alpha \sin(\omega_b t)} , \quad (16)$$

$$\sum_j \Theta(E_j)(ik_j)T_j e^{ik_j a}e^{-i\omega_j t} +\sum_j \Theta(-E_j)(-k_j)T_j' e^{-k_j a}e^{-i\omega_j t} =\sum_j (A_j\kappa_j e^{\kappa_j a}-B_j\kappa_j e^{-\kappa_j a})e^{-i\omega_j t}e^{-i\alpha \sin(\omega_b t)} . \quad (17)$$

Implicit relations for the coefficients can be found by multiplying Eqs. (14)–(17) by $e^{i\omega_n t}$ where $-\infty\leq\omega_n\leq\infty$. Integration over all time gives

$$\delta_{0,n}+\Theta(E_n)R_n+\Theta(-E_n)R_n'=\sum_j (A_j+B_j)I_{nj}(\alpha) , \quad (18)$$

$$ik_0\delta_{0,n}-\Theta(E_n)ik_nR_n+\Theta(-E_n)k_nR_n' = \sum_j (A_j\kappa_j - B_j\kappa_j)I_{nj}(\alpha) , \quad (19)$$

$$\Theta(E_n)T_n e^{ik_n a}+\Theta(-E_n)T_n' e^{-k_n a} = \sum_j (A_j e^{\kappa_j a}+B_j e^{-\kappa_j a})I_{nj}(\alpha) , \quad (20)$$

$$\Theta(E_n)ik_nT_n e^{ik_n a}-\Theta(-E_n)k_nT_n' e^{-k_n a} = \sum_j (A_j\kappa_j e^{\kappa_j a}-B_j\kappa_j e^{-\kappa_j a})I_{nj}(\alpha) , \quad (21)$$

where

$$I_{nj}(\alpha)=\int_{-\infty}^{\infty} e^{i(\omega_n-\omega_j)t}e^{-i\alpha\sin(\omega_b t)}dt . \quad (22)$$

The integral $I_{nj}(\alpha)$ may easily be solved by using the identities[7]

$$\cos(z\sin\theta)=J_0(z)+2\sum_{l=1}^{\infty}J_{2l}(z)\cos(2l\theta) ,$$

$$\sin(z\sin\theta)=2\sum_{l=0}^{\infty}J_{2l+1}(z)\sin[(2l+1)\theta] ,$$

where $J_l(z)$ are Bessel functions of integer order. This gives

$$I_{nj}(\alpha)=J_0(\alpha)\delta_{n,j}+\sum_{l=1}^{\infty}J_{2l}(\alpha)(\delta_{\omega_{nj},2l\omega_b}+\delta_{\omega_{nj},-2l\omega_b})+\sum_{l=0}^{\infty}J_{2l+1}(\alpha)(\delta_{\omega_{nj},(2l+1)\omega_b}-\delta_{\omega_{nj},-(2l+1)\omega_b}) , \quad (23)$$

where $\omega_{nj}\equiv\omega_n-\omega_j$. Equations (18)–(21) constitute an infinite set of linear equations from which the coefficients can be determined.

The solutions for the coefficients $(A_j,B_j,R_n,R_n',T_n,T_n')$ appearing in Eqs. (18)–(21) can be divided into two cases. In case 1, $E_n\neq E_0+N\omega_b$; $N=0,\pm1,\pm2,\pm3,\ldots$. This condition gives an infinite set of homogeneous equations which relates the unknown coefficients. The values for all the coefficients can be found trivially to equal zero for this case.

In case 2, where $E_n=E_0+N\omega_b$; $N=0,\pm1,\pm2,\pm3,\ldots$, an infinite set of inhomogeneous equations results for which a unique solution can, in principle, be found. As a matter of practical importance, the infinite set of equations may be reduced to a finite and solvable set of simultaneous equations by realizing that the coupling coefficients I_{nj} approach zero as $|n-j|$ becomes large. Therefore, by arbitrarily restricting the sum over j in Eqs. (18)–(21) to states with energies which lie between $E_0-j'\omega_b\leq E_n\leq E_0+j'\omega_b$, a set of $8j'+4$ complex simultaneous equations result. We typically find that a value of $j'\simeq6$ is sufficient for a converged calculation of the $(A_j,B_j,R_n,R_n',T_n,T_n')$ since $J_l(\alpha)\simeq0$ for $l\gtrsim6$ provided α is small. For large α, more equations must be incorporated and therefore sufficient computer time and memory must be available to solve the resulting equations.

From the discussion above, it should be evident that the wave function for, say, the transmitted wave can be rewritten as

$$\Psi_{\rm III}(x,t)=\sum_{n=-\infty}^{\infty}T_n\Theta(E_0+n\omega_b)e^{ik_nx}e^{-i(E_0+n\omega_b)t}+\sum_{n=-\infty}^{\infty}T_n'\Theta(-(E_0+n\omega_b))e^{-k_nx}e^{-i(E_0+n\omega_b)t} , \quad (24)$$

where $k_n=|E_0+n\omega_b|^{1/2}$ and where n is now restricted to the signed integers $0,\pm1,\pm2,\pm3,\ldots$. The important feature of this result is that the sum over continuous energies previously introduced in Eq. (5) is replaced with a sum over discrete energies centered about the incident energy E_0. This result will be used in the next subsection to discuss the calculation of the flux transmitted across the potential barrier.

C. Transmission and reflection probabilities

The transmission and reflection probabilities for the final states E_n can be found by defining the transmitted flux in the standard way[2]:

$$f_t(x,t)=-2\,\mathrm{Im}[\Psi_{\rm III}(x,t)\nabla\Psi_{\rm III}^*(x,t)] . \quad (25)$$

From this, the transmission probability τ is given by

$$\tau=f_t/f_0 \quad (26)$$

where $f_0=2k_0$ in our system of units.

It is useful to evaluate the transmitted flux explicitly for a simplified case, say a situation in which $\alpha\ll1$ such that the initial state will, to a good approximation, make transitions only to final states E_n given by $E_0\pm\omega_b$. Because of the properties of $I_{nj}(\alpha)$ under these conditions, the sums over j in Eqs. (18)–(21) can be restricted to values of $j=-1,0,1$. By assuming for sake of simplicity that $E_j>0$ for the range of final-state energies $E_0+j\omega_b$, it is easy to show by explicit evaluation of Eq. (25) that the transmitted flux is given by

$$f_t = 2(k_1 |T_1|^2 + k_0 |T_0|^2 + k_{-1} |T_{-1}|^2) + 2\,\mathrm{Im}[ik_1(T_0 T_1^* e^{i(k_0-k_1)x+i\omega_b t} + T_{-1} T_1^* e^{i(k_{-1}-k_1)x+i2\omega_b t}) + ik_0(T_1 T_0^* e^{i(k_1-k_0)x-i\omega_b t} + T_{-1} T_0^* e^{i(k_{-1}-k_0)x+i\omega_b t}) + ik_{-1}(T_1 T_{-1}^* e^{i(k_1-k_{-1})x-i2\omega_b t} + T_0 T_{-1}^* e^{i(k_0-k_{-1})x-i\omega_b t})] . \quad (27)$$

Since an incident quantum particle must eventually leave the barrier region, the sum of the time average of the reflection and transmission probabilities for the three states $E_0-\omega_b$, E_0, and $E_0+\omega_b$ leaving the barrier must equal unity. For the case under consideration this means that

$$\tau+\rho=\frac{k_1}{k_0}(|T_1|^2+|R_1|^2)+|T_0|^2+|R_0|^2 + \frac{k_{-1}}{k_0}(|T_{-1}|^2+|R_{-1}|^2)=1 , \quad (28)$$

where ρ, the reflection probability is defined in a way similar to Eq. (26). The result stated by Eq. (28) is a convenient criterion for determining if a sufficient number of terms have been included in Eqs. (18)–(21) when solving for the coefficients. The convergence of the sum of $\tau+\rho$ towards unity is illustrated in Fig. 2 which plots $1-(\rho+\tau)$ as a function of j', the number of terms included in the calculation of the coefficients. The parameters chosen for the calculation are rather extreme to clearly illustrate the convergence of the sum. As can be seen from the figure the convergence is entirely adequate for most purposes when $j'\simeq 6$, indicating that in this case, only states with final-state energies E_n such that $E_0-6\omega_b \le E_n \le E_0+6\omega_b$ will have a finite probability of being occupied.

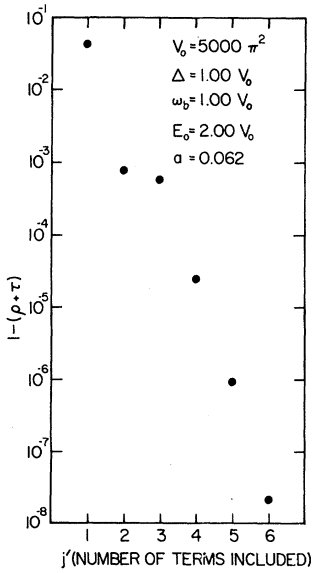

FIG. 2. Plot of the convergence toward unity of the sum of the time-averaged reflection and transmission probabilities for a time-dependent rectangular barrier described by the parameters listed. The abscissa plots the number of terms included in the calculation of the coefficients found in Eqs. (18)–(21).

For the particular case under discussion ($j=-1,0,1$), Eq. (27) only includes energies $E_n>0$, a realistic assumption so long as $E_0>\omega_b$ and α is small. If these conditions are violated, transitions to virtual states characterized by energies $E_n<0$ are possible. It is important to show that in this case, no transmitted or reflected flux escapes from the barrier region at these energies. When terms for $E_n<0$ are included in Eq. (24), it is simple to show that no time-independent contributions to the transmitted flux for these states results because Eq. (25) selects out only the imaginary part of the current density operator. The time averaged value of τ or ρ therefore will not include a contribution from these negative energies and therefore these states will not give rise to a transmitted or reflected flux. Furthermore, states with $E_n<0$ are localized to regions close to the potential barrier since the wave function for these states are exponentially damped with position. It therefore must follow that states with $E_n<0$ which are populated by the oscillating potential barrier remain localized near the barrier until they undergo a transition to a propagating state ($E_n>0$) and thereby leave the barrier region.

D. Interference effects

On the basis of the above calculation, it can be concluded that an oscillating potential barrier influences an incident quantum particle by inducing transitions from an initial state to final states which are quantized in energy units of ω_b, the frequency of the oscillating potential barrier. The transmitted flux leaving the barrier region exhibits a number of interesting features which merit further discussion.

Firstly, as can be seen from Eq. (27), the transmitted flux will acquire different velocity components as it leaves the barrier region. This result is in strong contrast to that found for the simple static

rectangular barrier in which the transmitted flux escapes from the barrier region at the same velocity as the incident flux. The different velocity components in the emitted flux is a direct consequence of the transitions to different final-state energies induced by the oscillating barrier. Because of this consideration, it can be expected that calculations of the dynamic transmission and reflection probabilities differ from the values obtained for the static barrier.

It is also apparent from the simplified case discussed above that the time-dependent potential barrier causes the transmitted flux to oscillate about the time-averaged value calculated from the first three terms of Eq. (27) so that, to a first approximation, the barrier acts as a quantum-mechanical shutter which modulates the emitted probability density at a frequency determined by ω_b. In addition, further modulation of the transmitted flux will result due to quantum-mechanical interference effects. This is clearly shown in Eq. (27) by the presence of terms like $e^{-i2\omega_b t}$ which give rise to an oscillation in the transmitted flux at twice the frequency at which the barrier oscillates. These higher frequencies result from the interference of two states that leave the barrier at the same final energy but which reach that energy in two different ways. The interference between two such states results because of the coherent nature in which transitions are made in our model for the potential barrier.

These interference effects can become important if, for instance, Δ/ω_b is allowed to have specific values. If $\Delta/\omega_b = 5.1356\ldots$, then $J_2(\Delta/\omega_b) \equiv 0$ and direct transitions from any state to any other state which is $\pm 2\omega_b$ different in energy will be forbidden, a consequence of the complete destructive interference in the probability amplitude for any state to change its energy by $\pm 2\omega_b$ under these conditions. When such a condition arises, the final state with energy $\pm\omega_b$ different from the incident state will have a maximum coupling coefficient, I_{nj}. This result follows from the well-known property of Bessel functions of integer order which states that if for some α_1, $J_n(\alpha_1)=0$, then $|J_{n-1}(\alpha_1)|$ has a local maximum.

A particularly interesting situation occurs if $\Delta/\omega_b = 2.4048\ldots$, since then $J_0(\Delta/\omega_b) \equiv 0$. Such a condition indicates that the transmitted state leaving the barrier region at the same energy as the initial state is completely decoupled from the initial state. The incident state is therefore resonantly destroyed upon entering the barrier region and any flux transmitted at the energy of the incident state is a result of transitions to different final states which are subsequently coupled back to the initial state. Results similar to these are also found in Ref. 3.

III. DYNAMIC INTERACTION OF A GAUSSIAN WAVE PACKET WITH AN OSCILLATING RECTANGULAR BARRIER

In the preceding section, a dynamic wave-matching procedure has been described that permits solutions for the final-state wave functions, and hence the transmission and reflection probabilities for a quantum state that interacts with a potential barrier whose height varies sinusoidally with time. The solution of this problem involves two simplifying assumptions:

(1) The incident particle has a well-defined energy and momentum and hence is completely delocalized in position space.

(2) The barrier oscillates for all times at the same frequency ω_b and with the same amplitude Δ. In addition it is further assumed that the state of the barrier cannot change even though the incident particle can interchange energy with the barrier during the interaction.

In this section, the restrictions placed on energy and momentum of the incident particle are relaxed and as a consequence the time evolution of a localized Gaussian wave packet can be studied.

Because of the delocalized nature of the incident state used in Sec. II it is difficult to relate the previous calculation to an analytic discussion of the motion of a Gaussian wave packet interacting with the potential barrier. In order to illustrate the dynamics of this interaction we present several computer-generated plots of a Gaussian wave-packet scattering from the potential barrier specified by Eq. (2). The calculations were performed using a modification of an algorithm employed by GSS that calculates the time evolution of a wave packet incident upon a time-independent potential barrier or well.[6] Since the algorithm is fully described in Ref. 6 we only discuss the modification required to perform the calculations presented in this paper. Following the discussion of the modification to the algorithm several calculations are shown and discussed.

A. Modification of the algorithm

The algorithm employed by GSS makes use of the evolution operator $U(t,t_0)$ which transforms a

wave function at time t_0 into the wave function at time t:

$$\psi(t)=U(t,t_0)\psi(t_0) . \tag{29}$$

For conservative systems the evolution operator is simply

$$U(t,t_0)=e^{-iH(t-t_0)} \tag{30}$$

where H represents the Hamiltonian for a conservative system. If the system is not conservative the general form of the operator U is needed. When Eq. (29) is substituted into Eq. (1) the evolution operator is found to satisfy the following relation:

$$i\frac{\partial}{\partial t}U(t,t_0)=H(x,t)U(t,t_0) . \tag{31}$$

Even though Eq. (31) can be formally manipulated to give

$$U(t,t_0)=e^{-i\int_{t_0}^{t}H(x,t')dt'} , \tag{32}$$

this, however, does not insure that a proper solution to Eq. (31) has been found since it does not properly take into account the operator nature of $H(x,t)$. It can be shown that Eq. (32) is a valid solution only if the following commutation relation holds[8]:

$$[H(x,t),U(t,t_0)]=0 . \tag{33}$$

Using the potential energy of Eq. (2) in Eq. (32) gives the following results:

$$U_{\rm I}(t,t_0)=U_{\rm III}(t,t_0)=e^{-iH_0(t-t_0)} , \tag{34}$$

$$U_{\rm II}(t,t_0)=e^{-i(H_0+V_0)(t-t_0)-i\alpha(\sin\omega_b t-\sin\omega_b t_0)} . \tag{35}$$

It is easy to verify that both forms for U in Eqs. (34) and (35) satisfy the commutation relation of Eq. (33) and therefore are acceptable time-evolution operators.

The algorithm of GSS expresses the wave function at a time $t+\delta$ in terms of the wave function at a time t by Eq. (30). For small time increments, δ, the Cayley form for the exponential operator of Eq. (30) is useful because of its Hermitian properties. Equation (29) can therefore be rewritten as

$$\psi(t+\delta)=\frac{1-\frac{1}{2}i\delta H}{1+\frac{1}{2}i\delta H}\psi(t) . \tag{36}$$

GSS developed a differencing scheme in order to solve this differential equation for $\psi(t+\delta)$ given $\psi(t)$ and a time-independent H. Since the evolution operators of Eq. (34) have the same form as Eq. (30), no modification of the algorithm is required for regions I and III. In region II, however, this is not the case and a minor modification of the algorithm is needed. In general, Eq. (35) cannot be expanded into the same form as Eq. (36) because the argument of the exponential in Eq. (35) can be very large even if δ is small. This difficulty can be circumvented in one of two possible ways:

(1) If $\omega_b\delta$ is small, $\sin[\omega_b(t+\delta)]$ can be rewritten as $\omega_b\delta\cos(\omega_b t)+\sin(\omega_b t)$ and using this fact, Eq. (35) can be expressed as

$$U_{\rm II}(t+\delta,t)\simeq e^{-i\delta H(x,t)} ,$$

where $H(x,t)$ is the full time-dependent Hamiltonian appropriate for region II. The evolution operator can now be approximated by the Cayley form as given in Eq. (36) and the differencing scheme used by GSS can be used without further modification provided δ is made sufficiently small.

(2) Since

$$[e^{-i(H_0+V_0)\delta},e^{-i\alpha\{\sin[\omega_b(t+\delta)]-\sin(\omega_b t)\}}]=0 ,$$

the evolution operator in Eq. (35) can be split into a product with the Cayley form used to approximate the time-independent part:

$$\psi(t+\delta)=\frac{1-\frac{1}{2}i\delta(H_0+V_0)}{1+\frac{1}{2}i\delta(H_0+V_0)} \times e^{-i\alpha\{\sin[\omega_b(t+\delta)]-\sin(\omega_b t)\}}\psi(t) .$$

The differencing scheme of GSS can now be used with the simple modification that

$$\psi(t)\rightarrow e^{-i\alpha\{\sin[\omega_b(t+\delta)]-\sin(\omega_b t)\}}\psi(t) .$$

The second method discussed above is preferred since no further restrictions are placed on the size of δ. It is interesting to note that a time-dependent potential barrier can be discussed either in terms of the full time-dependent Hamiltonian (method 1) or, equivalently, in terms of an additional time-dependent phase factor which modifies $\psi(t)$ (method 2). Calculations using both methods outlined give the same result provided $\omega\delta$ is chosen sufficiently small.

B. Initial conditions

As shown in the previous subsection the numerical algorithm developed by GSS can be used with little modification to generate computer plots of a

Gaussian wave packet interacting with the time-dependent potential of Eq. (2). We now describe our implementation of the algorithm that illustrates the time evolution of a Gaussian wave packet incident on the potential barrier of interest.

The time-dependent potential is located in the middle of a large well 2 units wide with infinitely high walls (see Fig. 3) to ensure that the wave function vanishes at $x=0$ and 2 as is required by the algorithm. The initial wave function is represented as a Gaussian wave packet initially centered at $x=0.75$ and moving to the right with average momentum $k_0=\sqrt{E_0}$:

$$\psi(x,0)=e^{ik_0x}e^{-(x-0.75)^2/2\sigma^2}, \tag{37}$$

where $\sigma=0.05$.

Because of the energy transitions discussed in Sec. II, we confine our Gaussian wave packet in a wider region than GSS in order to prevent spurious results that can arise from reflections at the infinitely high walls during the time over which the interaction takes place. Even though our calculations are carried out in the region between 0 and 2, the plots we present only show the region between 0.5 and 1.5. For ready comparison to the results of GSS, we use $|V_0|=5000\pi^2$ for the average value of the time-dependent potential barrier which has a width of 0.062 units. The amplitude and frequency of the barrier oscillation that we use are given as a fraction of this average potential.

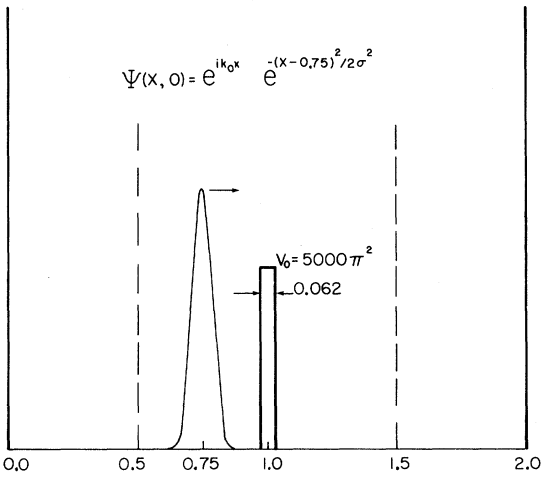

FIG. 3. Diagram illustrating the region in which the computer plots shown in Figs. 4–7 were generated. The time-dependent potential well or barrier is located in a larger well with infinitely high sides. The initial Gaussian wave packet is centered at $x=0.75$ and moves toward the barrier with average momentum $k_0=\sqrt{E_0}$. Only the region between the two dashed lines is shown in the computer plots presented in Figs. 4–7.

The maximum momentum allowed in the calculation as well as the position-step size, time-step size, and maximum barrier height are related by six constraints that are explicitly listed and explained by GSS and therefore will not be covered here. These constraints also indirectly limit the values of Δ and ω_b that can be used since a large α will force transitions to energy states that must be represented by large wave vectors in the final-state wave packets. The highest energy that can be reliably represented in these calculations then depends on the largest wave vector allowed which in turn depends on the position-step size used in the algorithm. For this reason, we have used a position-step size of $\epsilon=\frac{1}{2000}$ for all of our plots which means that the highest energy that can be reliably represented must be much less than $(2000\pi)^2$.

The position step size, ϵ, and time step size, δ, are related by $\lambda\equiv 2\epsilon^2/\delta=2.6k_0\times 10^{-3}$ where the value $2.6k_0\times 10^{-3}$ was chosen such that the reflected Gaussian for the static barrier case ($\Delta=\omega=0$) is approximately the same distance from the barrier at iteration 1400 as it was at $t=0$. In order to emphasize the effects of the time varying barrier, the barrier itself must undergo at least one full cycle of oscillation during the collision event. With this and the above considerations we use $0.5|V_0| \leq \omega_b \leq 1.5|V_0|$ and $\alpha \leq 0.5$.

C. Illustrative examples

The algorithm described by GSS was used with the appropriate time-evolution operators discussed in Sec. III A to generate a number of scattering events in which a Gaussian wave packet interacts with a time-dependent rectangular barrier. Computer plots of the probability density at different times during this interaction are presented for various initial parameters and the salient features of each event are discussed in turn.

In Fig. 4, we show two events, the first involves a time-dependent potential barrier[9] and the second involves a time-independent barrier included for sake of ready comparison. In each case the average barrier height is given by $V_0=5000\pi^2$ and the initial incident energy is $E_0=2V_0$. In Fig. 4, as in all following figures, the number of iterations used to obtain the graph in any given frame is included in the upper right-hand corner of that frame.

In Fig. 4(a) we show the time evolution of the Gaussian wave packet as it interacts with a poten-

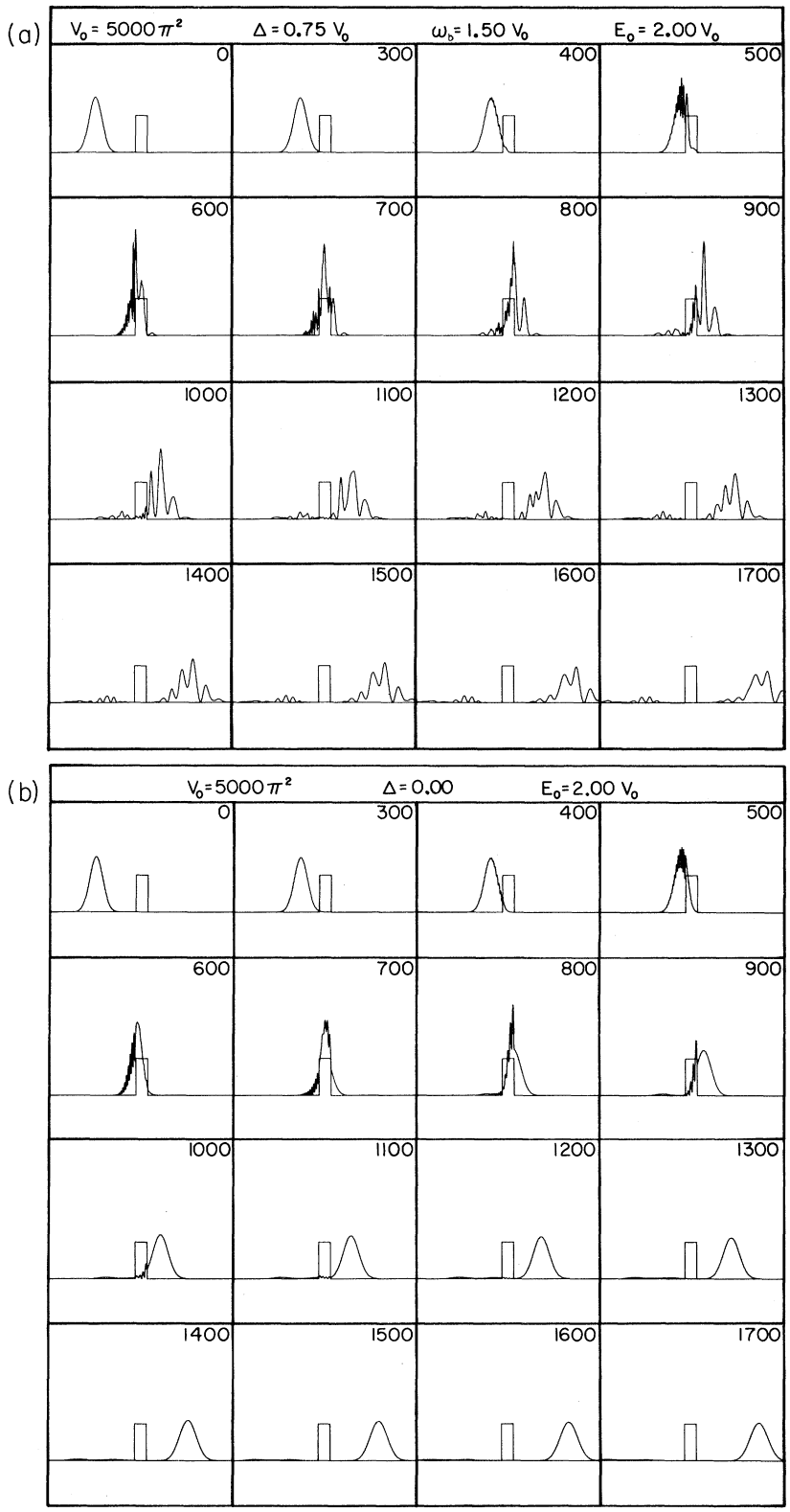

FIG. 4. Two plots which show the interaction of a Gaussian wave packet of initial average energy $E_0 = 2V_0$ with a potential barrier of average height $V_0 = 5000\pi^2$. In (a) $\omega_b = 1.5V_0$ with $\alpha = 0.5$; the barrier oscillates about once per frame. (b) is the corresponding static barrier case in which $\omega_b = 0$.

tial barrier that oscillates approximately one full cycle between each frame shown. To a first approximation the oscillating barrier acts like a shutter which emits a Gaussian-shaped wave packet once every complete cycle of the barrier's oscillation. This is clearly shown by the multipeaked nature of the time-evolving wave packets. Close inspection of this figure reveals that the initial packet emerging from the barrier has a higher average velocity than that observed for the time independent potential barrier shown in Fig. 4(b). This is clear evidence for the transitions to higher-energy states discussed in Sec. II.

In Fig. 5 we show the time evolution of a Gaussian wave packet as it interacts with a potential well whose depth varies as a function of time. The parameters in this particular figure were chosen so as to further emphasize that the transmitted wave packet is made up of wave vectors which are *not* present in the initial wave packet. This fact is indicated by the sequence of arrows shown in Fig. 5 which illustrate the splitting and eventual separation of the tallest peak in the transmitted wave packet. The splitting of this peak is direct evidence that the barrier has induced transitions to different energy states as described in Sec. II of this paper. A careful examination of Fig. 4(a) shows similar features.

Finally, in Fig. 6 we consider the case of a Gaussian wave packet interacting with a time-varying rectangular potential well that undergoes one complete oscillation about every two frames. As in all rectangular wells, at least one bound state will occur; for the well we have chosen, $V_0=5000\pi^2$, there are a total of five bound states. The purpose of this figure is to illustrate the effect of populating some of these bound states. The average initial energy of the incident wave packet and the frequency of oscillation of the barrier are chosen such that a downward transition of $-\omega_b$ in energy from the incident

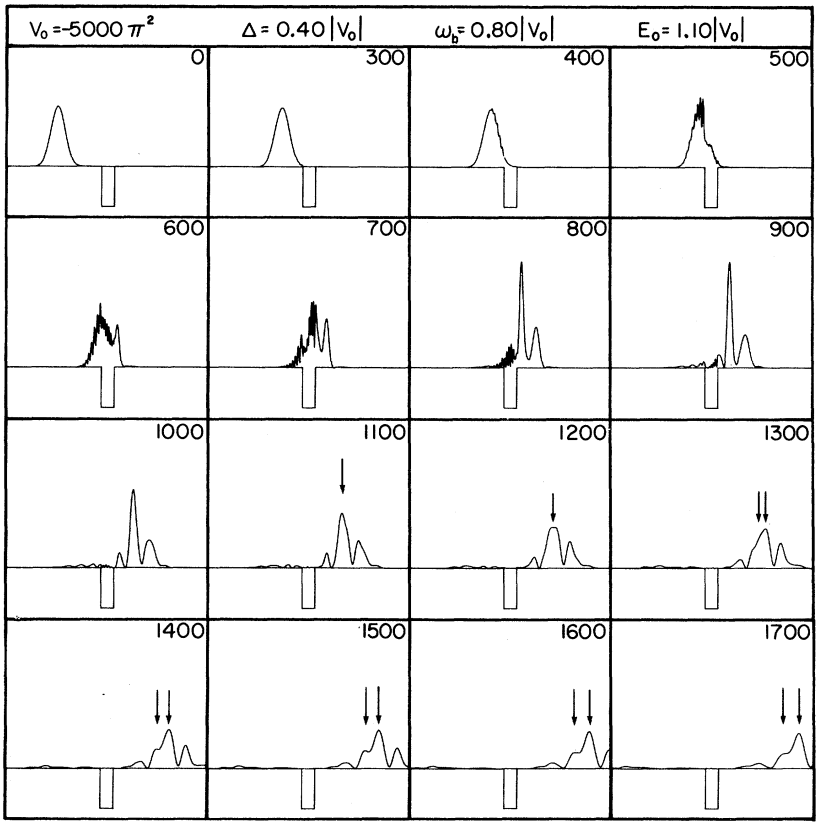

FIG. 5. Gaussian wave packet with average energy $E_0=1.1\,|\,V_0\,|$ incident on an oscillating well with $V_0=-5000\pi^2$, $\omega_b=0.8\,|\,V_0\,|$, and $\alpha=0.5$. This plot demonstrates that each Gaussian-shaped packet emitted from the barrier region is actually a superposition of two or more wave packets, each with a different average energy. This superposition is illustrated by the arrows which show the slow-moving packet (with average energy $E=E_0-\omega_b$) splitting off from one such Gaussian-shaped packet.

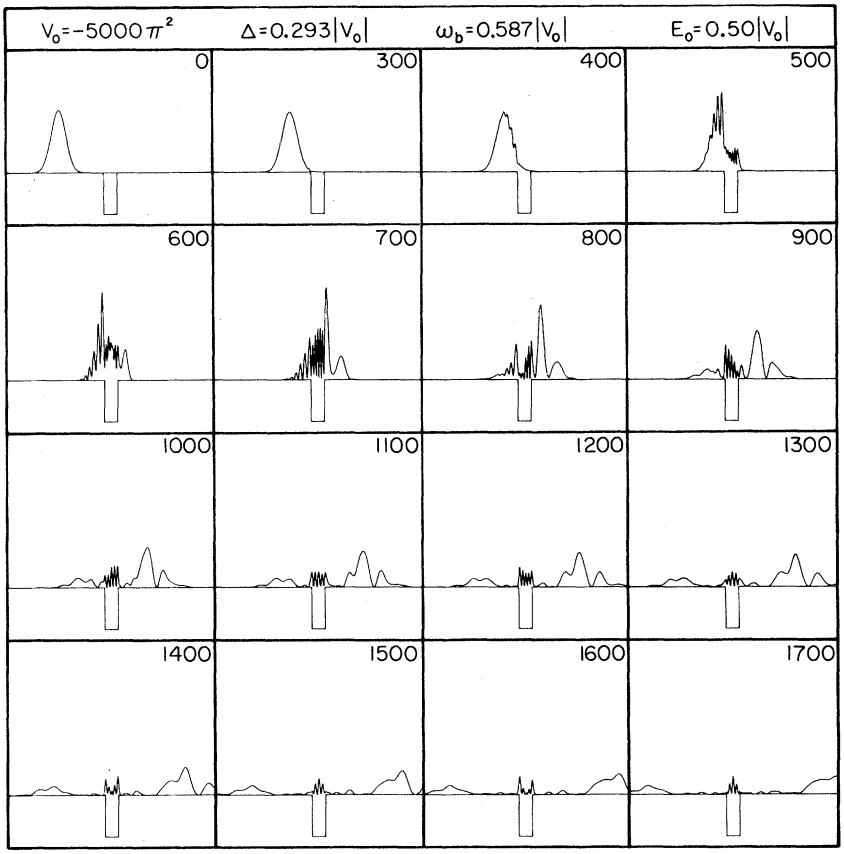

FIG. 6. Gaussian wave packet with energy $E_0=0.5\,|\,V_0\,|$ incident on oscillating potential well with average energy $V_0=-5000\pi^2$, $\omega_b=0.587\,|\,V_0\,|$, and $\alpha=0.5$. The value for ω_b was chosen so that the final-state energy of $E=E_0-\omega_b$ corresponds in energy with the highest bound state in the equivalent static well of depth $V_0=-5000\pi^2$. This bound state is at $E_{\text{bound}}=-4270$. This figure clearly shows that under these circumstances, there is a finite probability that the incident quantum particle can be captured in the well.

energy E_0 will exactly correspond to the bound state with highest energy. As is clear from the time evolution of the Gaussian packet, a finite probability for the quantum state to remain in the vicinity of the well is observed even after the transmitted and reflected wave packets are far from the region of the well. This is a somewhat surprising result since Δ, the amplitude of the oscillating barrier, is sufficiently large that the populated bound state is pushed into the continuum during the oscillation of the barrier. It is also clear from the figure that the bound state decays in time since small-amplitude packets are continually leaving the barrier region. This result is due to the upward transitions in energy that are induced by the time-dependent potential.

It is worth noting that for the particular parameters chosen in Fig. 6, a transition to an energy of $E_0-2\omega_b$ is close to a bound state located at the bottom of the well. Since the spread in energy of the incident Gaussian wave packet is sufficiently broad, this lower bound state will also become populated. However, the coupling coefficient for this process is much smaller than that for a transition to $E_0-\omega_b$. It is also for this reason that no bound states are observed to be occupied in Fig. 5.

D. Phasing considerations

Certain aspects of the calculations discussed above are particularly relevant to the physical processes involved in the photoemission of electrons from a metal surface in the presence of a high applied electric field. As discussed in Ref. 5, such experiments are thought to offer a particularly promising probe of the time-dependent formation of the image charge potential.[10–21] One crucial claim postulated in Ref. 5 was that the presence of an oscillating potential barrier will modulate the

transmission probability of an incident electron. It was assumed that the modulation of the transmission probability would be related to the phase of the oscillating barrier at the time the electron encountered the barrier region.

With the techniques discussed above, the importance of the phase of the oscillating barrier with respect to the position of the incident particle can be investigated. A calculation has been performed in which a Gaussian wave packet was directed onto an oscillating square potential barrier so that the Gaussian wave packet reached the barrier region at a time corresponding to the maximum and minimum heights of the potential. Figure 7 illustrates the interaction of a Gaussian wave packet with average energy $E_0=1.35V_0$ incident upon a square barrier. In this figure, the oscillatory barrier was described by

$$V=V_0+\Delta\cos(\omega_b t+\theta)\ ,$$

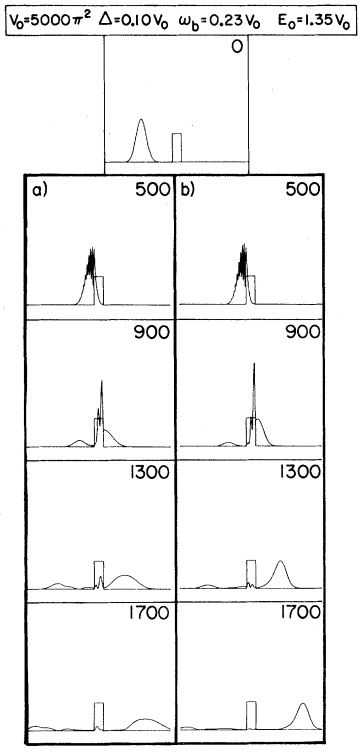

FIG. 7. Gaussian wave packet with energy $E_0=1.35V_0$ incident on an oscillating square barrier with $\omega_b=0.23V_0$. In (a), the barrier height is higher than its average value V_0 during the interaction time of the Gaussian packet, while in (b) the barrier height is lower than its average value during the interaction time. The resulting transmission probabilities are $T=0.71$ in (a) and $T=0.81$ in (b).

where ω_b is chosen so that the barrier undergoes $\sim\frac{1}{2}$ of a complete oscillation in the time it takes the Gaussian wave packet to cross the barrier region. The phase angle θ is adjusted so that in Fig. 7(a), the wave packet begins to interact with the square barrier when $\omega_b t+\theta\simeq 7\pi/4$. This condition ensures that during the interaction, the barrier has a height greater than its time-averaged value. In Fig. 7(b), $\omega_b t+\theta\simeq 3\pi/4$ at the time the wave packet begins to interact with the barrier so that the barrier has a height less than its time-averaged value. The resulting transmission probabilities calculated from the last frames in this figure show that for Fig. 7(a), $T=0.71$ while for Fig. 7(b), $T=0.81$.[22]

The 12% change in the transmission probability found in this model calculation appears to justify the hypothesis suggested in Ref. 5, that an electron escaping from a metal surface in the presence of a high electric field can have its transmission probability altered by the time evolution of the image potential. Even though our calculations have not been performed for a potential barrier with a realistic shape, the qualitative conclusions drawn from this model calculation still seem appropriate, namely that the transmission probability depends critically on the phase of the oscillating barrier at the time when a Gaussian wave packet interacts with it.

IV. DISCUSSION AND CONCLUSIONS

In this paper we have derived the dynamic transmission and reflection probability for a quantum particle that interacts with a rectangular barrier oscillating sinusoidally with time. The salient feature of our calculations is that the barrier induces transitions from the incident energy to energies which differ by integer multiples of the barrier frequency. In addition the transmitted probability density of the quantum state is also modulated in time at integer multiples of the frequency of the oscillating barrier. The calculations performed for a delocalized particle have been extended to a localized Gaussian wave packet incident on an oscillating barrier. In this case, the barrier also induces transitions to other energies and modulates the transmitted probability density in ways similar to that for the delocalized incident particle. Furthermore, the transmission probability under these circumstances is also found to depend on the phase of the oscillating barrier when the Gaussian packet interacts with it.

Methods are being developed to extend these calculations to barriers which depend on position and

time in a more complicated way than that described in this paper. In addition, models are sought for potential barriers characterized by a time dependence that is a result of the virtual excitations of a quantum system like the surface-plasmon modes of a metal surface. Such a feature would be particularly useful for a realistic calculation of tunneling through a potential barrier influenced by the dynamic image potential.

ACKNOWLEDGMENTS

This work is supported by the United States Department of Energy under Grant No. DE-AC02-79ER10464. The authors wish to thank A. W. Overhauser for many helpful discussions throughout the course of this work and T. E. Clark and C. M. Egert for their critical comments during the initial stages of this project.

---

[1]Throughout this paper we will use the words potential barrier to also describe a quantum-mechanical potential well.

[2]See for example, A. Messiah, *Quantum Mechanics* (Wiley, New York, 1968).

[3]E. Evans and D. L. Mills, Phys. Rev. B 7, 853 (1973).

[4]T. E. Sullivan and P. H. Cutler, Surf. Sci. 62, 455 (1977).

[5]R. Reifenberger, D. L. Haavig, and C. M. Egert, Surf. Sci. 109, 276 (1981).

[6]A. Goldberg, H. M. Schey, and J. L. Schwartz, Am. J. Phys. 35, 177 (1967).

[7]*Handbook of Mathematical Functions,* edited by M. Abramowitz and I. A. Stegun (Dover, New York, 1970), p. 361.

[8]C. Cohen-Tannoudji, B. Diu, and F. Laloë, *Quantum Mechanics* (Wiley, New York, 1977), pp. 308–311.

[9]The sinusoidal variation in height of the potential barrier is not shown in Figs. 4–7.

[10]D. M. Newns, Phys. Rev. B 1, 3304 (1970).

[11]R. H. Ritchie, Phys. Lett. 38A, 189 (1972).

[12]R. Ray and G. D. Mahan, Phys. Lett. 42A, 301 (1972).

[13]J. Harris and R. O. Jones, J. Phys. C 6, 3585 (1973).

[14]D. Chan and P. Richmond, Surf. Sci. 39, 437 (1973).

[15]J. Heinrichs, Phys. Rev. B 8, 1346 (1973).

[16]J. Harris and R. O. Jones, J. Phys. C 7, 3751 (1974).

[17]G. D. Mahan, in *Collective Properties of Physical Systems Nobel Symposium XXIV,* edited by B. I. Lundquist and S. Lundquist (Academic, New York, 1974).

[18]R. G. Barrera and C. B. Duke, Phys. Rev. B 13, 4477 (1976).

[19]D. L. Mills, Phys. Rev. B 15, 763 (1977).

[20]M. Jonson, Solid State Commun. 33, 743 (1980).

[21]P. M. Echenique, R. H. Ritchie, N. Barberan, and John Inkson, Phys. Rev. B 23, 6486 (1981).

[22]The small probability density located in the barrier region has not been included in this calculation for T. In Fig. 7(a), this trapped probability density is found to be $\sim 3\%$ of the area of the incident wave packet.